magnetic resonance, because the incident electric field cannot couple to the capacitance of the LC circuit. This argument is also true for the vertical polarization.

Figure 4 shows the effective permeability μ and the effective permittivity ε around the LC resonance, retrieved from the computed scattering data for two different orientations of the SRRs with respect to the incident wave (*13*). Figure 4A corresponds to the spectra shown on Fig. 3A, where only the electric field can couple to the LC resonance (*8*). In this case we obtain an electric resonant response in ε, accompanied by a simultaneous antiresonant behavior in μ (*14*). The retrieved data for the other polarization (Fig. 3B) exhibits no structure in ε and μ in this frequency range (*11*). In Fig. 4B, the beam configuration is such that the magnetic field can couple to the LC resonance, whereas the electric field cannot. For this polarization, a magnetic resonant response in μ is obtained with a negative value of μ in the 85-THz region. This is an important precondition for the realization of a metamaterial with a negative index of refraction. The retrieved ε exhibits an antiresonant behavior in this case (*14*).

Our results have two important consequences. First, usual ferromagnetic and antiferromagnetic resonances tend to die out above gigahertz frequencies. Thus, one can usually safely assume that the magnetic permeability of optical materials is unity. In other words, the optical properties of materials are exclusively determined by the optical polarization; the optical magnetization is zero. This is no longer true for the metamaterials presented here, enabling interesting new effects in linear optics as well as in nonlinear optics. Indeed, additional theoretical calculations show that the local fields within the gap of the LC circuit can be orders of magnitude larger than in free space or in bulk, which potentially enhances nonlinear effects and conversion efficiencies considerably. Second, a negative magnetic permeability would allow for negative-index materials at optical frequencies, which seemed totally out of reach just a few years ago.

References and Notes

1. R. A. Shelby, D. R. Smith, S. Schultz, *Science* **292**, 77 (2001).
2. V. G. Veselago, *Sov. Phys. Usp.* **10**, 509 (1968).
3. J. B. Pendry, *Phys. Rev. Lett.* **85**, 3966 (2000).
4. D. R. Smith, W. J. Padilla, D. C. Vier, S. C. Nemat-Nasser, S. Schultz, *Phys. Rev. Lett.* **84**, 4184 (2000).
5. D. R. Smith, S. Schultz, P. Markos, C. M. Soukoulis, *Phys. Rev. B* **65**, 195104 (2002).
6. T. Koschny, M. Kafesaki, E. N. Economou, C. M. Soukoulis, *Phys. Rev. Lett.* **93**, 107402 (2004).
7. C. Sirtori, *Nature* **417**, 132 (2002).
8. N. Katsarakis, T. Koschny, M. Kafesaki, E. N. Economou, C. M. Soukoulis, *Appl. Phys. Lett.* **84**, 2943 (2004).
9. D. R. Smith, J. B. Pendry, M. C. K. Wiltshire, *Science* **305**, 788 (2004).
10. T. J. Yen *et al.*, *Science* **303**, 1494 (2004).
11. S. Linden *et al.*, data not shown.
12. M. A. Ordal *et al.*, *Appl. Opt.* **22**, 1099 (1983).
13. D. R. Smith, S. Schultz, P. Markos, C. M. Soukoulis, *Phys. Rev. B* **65**, 195104 (2002).
14. T. Koschny, P. Markos, D. R. Smith, C. M. Soukoulis, *Phys. Rev. E* **68**, 065602 (2003).

15. We acknowledge the support by the Center for Functional Nanostructures (CFN) of the Deutsche Forschungsgemeinschaft (DFG) within project A.1.4. The research of M.W. is further supported by the DFG-Leibniz award 2000 and that of C.M.S. by the Alexander von Humboldt senior-scientist award 2002, by Ames Laboratory (contract no. W-7405-Eng-82), European Union Future and Emerging Technologies project, Development and Analysis of Left-Handed Metamaterials, and Defense Advanced Research Projects Agency (contract no. MDA 972-01-2-0016).

Supporting Online Material

www.sciencemag.org/cgi/content/full/306/5700/1351/DC1
SOM Text

17 September 2004; accepted 20 October 2004

A Chiral Route to Negative Refraction

J. B. Pendry

Negative refraction is currently achieved by driving the magnetic permeability and electrical permittivity simultaneously negative, thus requiring two separate resonances in the refracting material. The introduction of a single chiral resonance leads to negative refraction of one polarization, resulting in improved and simplified designs of negatively refracting materials and opening previously unknown avenues of investigation in this fast-growing subject.

Negative refraction is an intriguing and counterintuitive phenomenon that has attracted much attention. Not only does light bend the "wrong" way at a normal/negative interface, but there are even more surprising properties, such as the ability to construct a "perfect" lens for which the resolution is limited not by the wavelength but by the quality of manufacture (*1*, *2*). Negative refraction never occurs in nature, and we rely on artificial materials, metamaterials, to realize the effect as discussed in (*3*). In this paper, I discuss the consequences of chirality and show that it offers an alternative to the present routes to negative refraction. I produce a practical design that is chiral, has many advantages, and exhibits novel properties.

In the original description of negative refraction (*4*), it was stated that when the electrical permittivity and magnetic permeability are both negative light bends the wrong way at an interface. It was only much later, with the ability to construct artificial metamaterials, that the properties could be realized (*5*–*7*): The original prescription for a subwavelength array of thin metallic wires combined with resonant metallic rings has been extensively investigated, and negative refraction at microwave frequencies has been confirmed by several investigators (*8*–*13*). Although referred to as "left-handed" materials, I stress that the sense in which this term was used has nothing to do with chirality. Therefore I prefer to use the expression "negatively refracting" to avoid confusion.

The nonchiral designs suffer some limitations. They use two sets of resonant structures, one for the electric and the other for the magnetic response, and these structures have to be very carefully designed to resonate in the same frequency range. Figure 1 shows a typical schematic band structure where it was assumed that

$$\mu < 0, \omega_1 > \omega > \omega_3$$
$$\varepsilon < 0, \omega_2 > \omega > \omega_4 \quad (1)$$

where μ is the magnetic permeability, ω is the frequency, and ε is the effective electric permittivity. The negatively dispersing band between ω_2 and ω_3 is responsible for a negative refractive index. The structure of the metamaterial is required to be as fine as possible so that the fields experience an effectively homogeneous material. The pres-

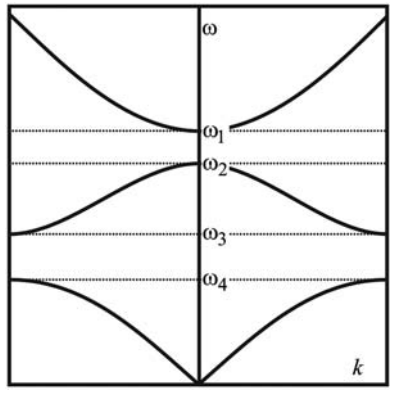

Fig. 1. Dispersion in a negatively refracting material: Typically two stop bands, $\omega_1 > \omega > \omega_2$ and $\omega_3 > \omega > \omega_4$, and a band of negative dispersion and hence of negative refraction, $\omega_2 > \omega > \omega_3$, are seen. In addition, there are two longitudinal modes (not shown), one magnetic in character and the other electric.

Department of Physics, Blackett Laboratory, Imperial College London, London SW7 2AZ, UK.

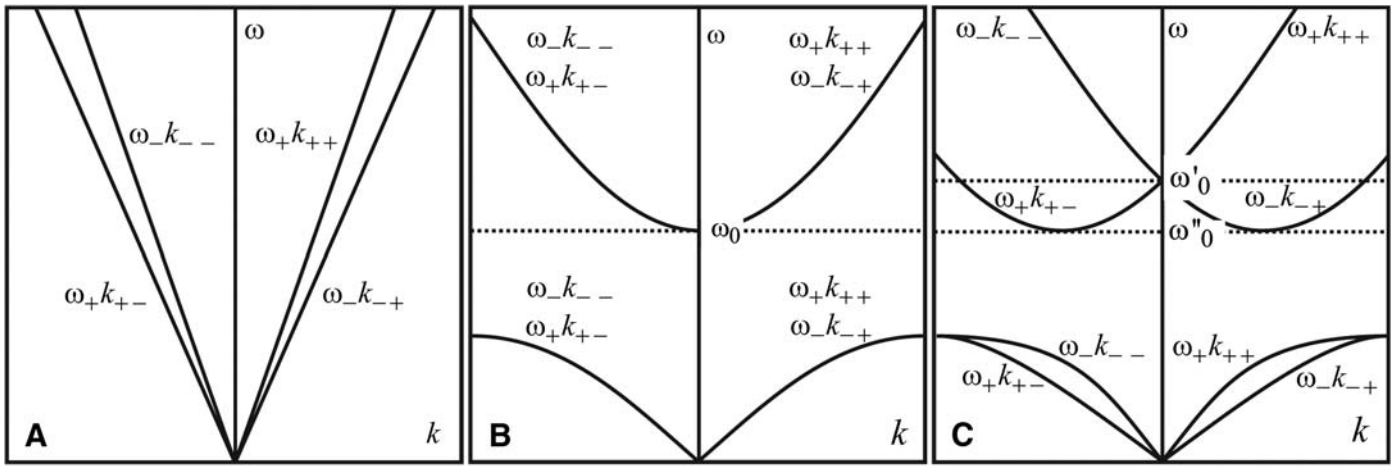

Fig. 2. (**A**) Dispersion of ω versus k in a homogeneous and isotropic chiral medium showing the two polarizations as nondegenerate. The subscripts on k refer first to the polarization and second to the sign of the group velocity. In this convention, polarization is positive if the projection of the photon spin on the z axis is positive. It does not refer to the projection of spin onto the wave vector. (**B**) Dispersion in a homogeneous and isotropic medium containing a set of resonant electric dipoles. Note the gap opened up where the permittivity is negative and the two degenerate transverse modes. There is an additional longitudinal mode, not shown, degenerate with the longitudinal modes at ω_0. (**C**) Introducing the resonant dipoles into a chiral medium splits the resonant transverse bands and results in a range of frequencies below ω_0' in which negative refraction can be seen for one of the polarizations. The longitudinal mode, again not shown, is degenerate with the transverse modes at ω_0'.

ent generation of designs go some way to achieving this but rarely do better than a wavelength-to-structure ratio of 10:1. Also, producing a magnetic resonance at optical frequencies will be particularly difficult if low loss is required.

Chiral materials exhibit a different refractive index for each polarization. The dispersion of wave vector, k, with ω is shown (Fig. 2A). Formally speaking we introduce a tensor, χ,

$$\chi_A = \begin{bmatrix} \chi_{EE} & \chi_{EH} \\ \chi_{HE} & \chi_{HH} \end{bmatrix} \quad (2)$$

which defines the response of the medium to an electromagnetic field:

$$\mathbf{D} = \chi_{EE}\mathbf{E} + \chi_{EH}\mathbf{H}$$
$$\mathbf{B} = \chi_{HE}\mathbf{E} + \chi_{HH}\mathbf{H} \quad (3)$$

where **D** is the electric displacement vector; **E**, the electric field intensity; **B**, the magnetic induction field; and **H**, the magnetic field intensity. The Supporting Online Material (SOM) Text relates χ to ω(k).

Next, consider another medium filled with resonant electric dipoles so that

$$\chi_B(\omega) = \begin{bmatrix} \left(1+\frac{\alpha^2}{\omega_0^2-\omega^2}\right) & 0 \\ 0 & 1 \end{bmatrix} \quad (4)$$

The response is shown in Fig. 2B. The resonance induces a band gap: a range of frequencies in which the electrical permittivity is negative and where there are no allowed states. The medium is not chiral, so the two transverse polarizations are degenerate. In addition to the transverse modes there is a single longitudinal mode, which is degenerate with the longitudinal modes at $k = 0$ and $\omega = \omega_0$.

Now consider what happens if dipole resonators are inserted into the chiral medium. The combined response is given by

$$\chi_C = \begin{bmatrix} \left(\chi_{EE} + \frac{\alpha^2}{\omega_0^2-\omega^2}\right) & \chi_{EH} \\ \chi_{HE} & \chi_{HH} \end{bmatrix} \quad (5)$$

and the schematic dispersion is plotted (Fig. 2C). Chirality splits the degenerate transverse modes and in doing so creates a range of frequencies just below ω_0' where the group velocity,

$$v_g = \partial\omega/\partial k \quad (6)$$

has the opposite sign to the phase velocity,

$$v_p = \omega/k \quad (7)$$

but only for one polarization. This is the signature of negative refraction. One can define a refractive index for each polarization,

$$n_\pm(\omega) = c_0 k_{\pm+}/\omega \quad (8)$$

where c_0 is the velocity of light in free space, and one of them is negative. An impedance can also be defined (SOM Text).

The bands shown in Fig. 2C are remarkable in several ways. In contrast to the nonchiral situation where there are two resonances and therefore two gaps, here there is only one gap. Hence, the transition to negative refraction is smooth and continuous at ω_0' with no gap. Only a chiral material can achieve this because it requires that the intersecting bands at $k = 0$ do not hybridize as they normally would do. Also, the bands at this point have finite group velocity but infinite phase velocity. For the chiral material, the minimum frequency, ω_0'', occurs as a finite wave vector, and hence the density of states diverges at this frequency.

In general when light in a vacuum is incident upon a slab of the new resonant chiral material, two refracted beams will be observed because a refracting surface can mix polarizations. However suppose the parameters are chosen such that

$$n_+ = -1 \quad (9)$$

and

$$Z_+ = +Z_0 \quad (10)$$

where Z_0 is the ratio of electric to magnetic fields for waves in the vacuum, that is, the impedance of the vacuum, and Z_+ is the ratio of electric to magnetic fields in the medium for the polarization that shows negative refraction (SOM Text). Then detailed calculations show that the slab is perfectly transparent to the + polarization. All the properties predicted for an isotropic nonchiral medium with

$$\varepsilon = -1, \ \mu = -1 \quad (11)$$

will be reproduced in this new medium but only for one of the polarizations. This includes the ability to focus the near fields and hence reproduce an image with resolution unlimited by wavelength.

This recipe for chiral negative refraction is a general one. Only the ingredients of a resonant system producing a band gap and chirality are needed. A moment's study of Fig. 2C will show that any minimum in ω(k) at $k = 0$ will produce negative refraction when split in this way.

Next I suggest a practical realization of a resonant chiral structure. I do this by

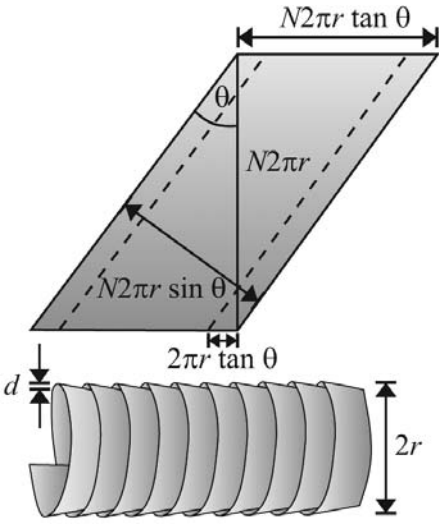

Fig. 3. Design for a chiral material. Continuous insulated strips of metal are wound in a helix and then individual coils are stacked in a three-dimensional log pile to make an isotropic structure.

winding a continuous insulated metal tape onto a cylinder so that it forms an overlapping helix (Fig. 3). More details of the performance of this structure are available (figs. S8 to S13). This is a chiral variant of the so-called Swiss roll structure used to produce negative permeability in the MHz range of frequencies (*14*). The structure is resonant because of inductance in the coiled helix and capacitance between the inner and outer layers of the helix. When current flows along the helix, not only does it produce a magnetic polarization along the axis, but it also produces an electric polarization because some of the current flows parallel to the axis. Typical values for the parameters are

$$r = 5 \times 10^{-3}\ \text{m}$$
$$a = 2 \times 10^{-2}\ \text{m},\ d = 1 \times 10^{-4}\ \text{m}$$
$$\theta = 5^\circ,\ N = 10 \qquad (12)$$

where a is the lattice constant of the log-pile structure and r, d, θ, and N are defined in Fig. 3. These parameters give negative refraction at around 100 MHz. The design can be tuned over a wide range of frequencies (SOM Text). Achieving strong chirality in the optical region of the spectrum is more difficult, but some promising design studies have been made (*15*).

The class of negatively refracting materials introduced here with the prescribed properties should open previously unknown avenues of investigation. Specific designs are greatly simplified with very compact internal structure, typically on a scale less than 1/100th of the free space wavelength at the resonant frequency. The structures offer further opportunities to extend the negative refraction concept.

References and Notes

1. J. B. Pendry, *Phys. Rev. Lett.* **85**, 3966 (2000).
2. J. B. Pendry, S. A. Ramakrishna, *J. Phys. Cond. Matter* **15**, 6345 (2003).
3. D. R. Smith, J. B. Pendry, M. C. K. Wiltshire, *Science* **305**, 788 (2004).
4. V. G. Veselago, *Soviet Physics Usp.* **10**, 509 (1968).
5. J. B. Pendry, A. J. Holden, W. J. Stewart, I. Youngs, *Phys. Rev. Lett.* **76**, 4773 (1996).
6. J. B. Pendry, A. J. Holden, D. J. Robbins, W. J. Stewart, *IEEE Trans. Microwave Theory Tech.* **47**, 2075 (1999).
7. D. R. Smith, W. J. Padilla, D. C. Vier, S. C. Nemat-Nasser, S. Schultz, *Phys. Rev. Lett.* **84**, 4184 (2000).
8. A. A. Houck, J. B. Brock, I. L. Chuang, *Phys. Rev. Lett.* **90**, 137401 (2003).
9. A. Grbic, G. V. Eleftheriades, *Phys. Rev. Lett.* **92**, 117403 (2004).
10. P. V. Parimi *et al.*, *Phys. Rev. Lett.* **92**, 127401 (2004).
11. E. Cubukcu, K. Aydin, E. Ozbay, S. Foteinopoulou, C. M. Soukoulis, *Nature* **423**, 604 (2003).
12. P. V. Parimi, W. T. Lu, P. Vodo, S. Sridhar, *Nature* **426**, 404 (2003).
13. E. Cubukcu, K. Aydin, E. Ozbay, S. Foteinopolou, C. M. Soukoulis, *Phys. Rev. Lett.* **91**, 207401 (2003).
14. M. C. K. Wiltshire *et al.*, *Science* **291**, 849 (2001).
15. Y. Svirko, N. Zheludev, *Appl. Phys. Lett.* **78**, 498 (2001).
16. I thank the Donostia International Physics Center (DIPC) for their hospitality during the course of this work; the Engineering and Physical Sciences Research Council for a senior fellowship; and the European Commission (EC) under project FP6-NMP4-CT-2003-505699, the U.S. Department of Defense/Office of Naval Research Multidisciplinary University Research Initiative grant N00014-01-1-0803, and the EC Information Societies Technology (IST) program Development and Analysis of Left-Handed Materials (DALHM) project number IST-2001-35511 for financial support.

Supporting Online Material
www.sciencemag.org/cgi/content/full/306/5700/1353/DC1
SOM Text
Figs. S1 to S13

15 June 2004; accepted 1 September 2004

Hertz-Level Measurement of the Optical Clock Frequency in a Single $^{88}Sr^{+}$ Ion

H. S. Margolis,* G. P. Barwood, G. Huang, H. A. Klein, S. N. Lea, K. Szymaniec, P. Gill

The frequency of the 5s $^2S_{1/2}$–4d $^2D_{5/2}$ electric quadrupole clock transition in a single, trapped, laser-cooled $^{88}Sr^{+}$ ion has been measured by using an optical frequency comb referenced to a cesium fountain primary frequency standard. The frequency of the transition is measured as 444,779,044,095,484.6 (1.5) hertz, with a fractional uncertainty within a factor of 3 of that of the cesium standard. Improvements required to obtain a cesium-limited frequency measurement are described and are expected to lead to a $^{88}Sr^{+}$ optical clock with stability and reproducibility exceeding that of the primary cesium standard.

Accurate time and frequency measurement is a long-standing requirement of science and technology, with applications including the realization of the Système International (SI) base units of time and length, satellite-based navigation and ranging, precision measurements of fundamental constants, and tests of physical theories (*1*). Since 1967, the internationally agreed definition of the second has its basis in the ground-state hyperfine transition in the ^{133}Cs atom at 9,192,631,770 Hz, and Cs fountain primary frequency standards now have reproducibilities of around 1 part in 10^{15} (*1*). Recent studies have indicated the potential of optical frequency standards based on high-Q transitions in laser-cooled trapped ions or atoms to achieve even better stabilities and accuracies (*2*, *3*). Combined with optical frequency measurement techniques based on femtosecond combs (*4*, *5*), these transitions may be used as practical frequency standards generating a direct microwave output (*3*), raising the possibility of a future redefinition of the SI second. To assess the suitability of an optical standard as the basis for such a new definition, it is important to make accurate measurements of its frequency relative to the Cs standard and to evaluate its reproducibility. In the medium term, this would allow such standards to be used as secondary representations of the second, contributing to International Atomic Time (TAI).

An important class of optical frequency standards are those that have their basis in narrow-linewidth forbidden transitions in single laser-cooled trapped ions, such as $^{199}Hg^{+}$ (*2*), $^{171}Yb^{+}$ (*6*, *7*), $^{115}In^{+}$ (*8*), and $^{88}Sr^{+}$ (*9*, *10*). The best previously reported frequency measurements are for the $^{199}Hg^{+}$ standard at 282 nm (*11*) and the $^{171}Yb^{+}$ standard at 435 nm (*6*), with quoted uncertainties of 1 part in 10^{14}. We present a measure-

National Physical Laboratory (NPL), Teddington, Middlesex TW11 0LW, UK.

*To whom correspondence should be addressed. E-mail: helen.margolis@npl.co.uk